nature neuroscience

Retrograde regulation of synaptic vesicle endocytosis and recycling

Kristina D Micheva[1], JoAnn Buchanan[1], Ronald W Holz[2] & Stephen J Smith[1]

Sustained release of neurotransmitter depends upon the recycling of synaptic vesicles. Until now, it has been assumed that vesicle recycling is regulated by signals from the presynaptic bouton alone, but results from rat hippocampal neurons reported here indicate that this need not be the case. Fluorescence imaging and pharmacological analysis show that a nitric oxide (NO) signal generated postsynaptically can regulate endocytosis and at least one later step in synaptic vesicle recycling. The proposed retrograde pathway involves an NMDA receptor (NMDAR)-dependent postsynaptic production of NO, diffusion of NO to a presynaptic site, and a cGMP-dependent increase in presynaptic phosphatidylinositol 4,5-biphosphate (PIP2). These results indicate that the regulation of synaptic vesicle recycling may integrate a much broader range of neural activity signals than previously recognized, including postsynaptic depolarization and the activation of NMDARs at both immediate and nearby postsynaptic active zones.

At chemical synapses, presynaptic electrical signals elicit postsynaptic responses via an intermediary secreted neurotransmitter. Chemical synapses are thus fundamentally asymmetric. It has recently become clear, however, that transmission is not strictly unidirectional: a variety of feedback signals flowing from postsynaptic origin toward presynaptic targets have been identified. The expanding list of possible retrograde signals now includes neurotrophins, nitric oxide (NO), cell–cell adhesion molecules, Eph receptors/ephrins and endocannabinoids[1,2]. Retrograde signaling has been implicated in various aspects of synaptic development and function, including synapse formation, maintenance and plasticity.

The generation of an NMDAR-dependent, retrograde NO signal has been studied extensively, due to its possible involvement in regulation of neuronal excitability and in memory processes[3]. It has been shown that NO can evoke or enhance neurotransmitter release[4–7], but little is known of the mechanisms of synaptic NO action. Recently, we discovered that postsynaptically generated NO can induce an increase in presynaptic PIP2, especially at synapses with high levels of vesicle recycling[8]. Numerous studies implicate PIP2 in the regulation of endocytosis and subsequent synaptic vesicle recycling[9–11], suggesting that a retrograde NO signal might regulate synaptic vesicle recycling via its action on PIP2.

To address the potential involvement of retrograde NO signals in the regulation of synaptic vesicle endocytosis and recycling, we used cultured hippocampal neurons. In these cells, NMDA receptors and nitric oxide synthase (NOS) have postsynaptic localization[12–14], and a functional retrograde NO pathway has been described previously[4,8]. The activation of postsynaptic NMDARs leads to an influx of Ca^{2+} ions, which bind to calmodulin and lead to the activation of NOS. Both the neuronal and endothelial isoforms of NOS are present in the hippocampus and may be contributing to the production of NO[15]. NO diffuses readily across cellular membranes and enters presynaptic sites, activating a variety of signaling cascades[3]. In the present study, we provide evidence that postsynaptically generated NO can regulate the speed of synaptic vesicle endocytosis and recycling, processes that until now have been linked only to presynaptic activity[16]. The proposed retrograde pathway involves a cGMP-dependent increase in presynaptic PIP2. Our experiments furthermore suggest that this signaling pathway may regulate the strength of synaptic transmission under conditions of continuous synaptic activity.

RESULTS

To visualize synaptic vesicle endocytosis, neurons were transfected with a cDNA construct encoding VAMP2/synaptobrevin fused to GFP (VAMP–GFP). The fusion protein is oriented such that GFP is within the acidic lumen of synaptic vesicles. Because of its pH sensitivity, GFP fluorescence increases upon exocytosis when VAMP–GFP becomes exposed to the neutral extracellular pH. Subsequent endocytosis of synaptic vesicles is reported quantitatively by a decrease in GFP fluorescence, caused by internalization of VAMP–GFP within endocytic vesicles and their rapid acidification[17]. Active presynaptic boutons were also identified and analyzed using the fluorescent dye FM 4-64. When applied extracellularly during periods of synaptic activity, FM 4-64 becomes trapped within recycled synaptic vesicles (FM loading) and can be visualized by fluorescence microscopy after washing off extracellular dye. Subsequent exocytosis causes release of the dye (FM unloading)[18]. Changes in FM 4-64 fluorescence of hippocampal

[1]Department of Molecular and Cellular Physiology, Stanford University, Stanford, California 94305, USA. [2]Department of Pharmacology, University of Michigan Medical School, Ann Arbor, Michigan 48109, USA. Correspondence should be addressed to KDM (kmicheva@stanford.edu).

Published online 10 August 2003; doi:10.1038/nn1114

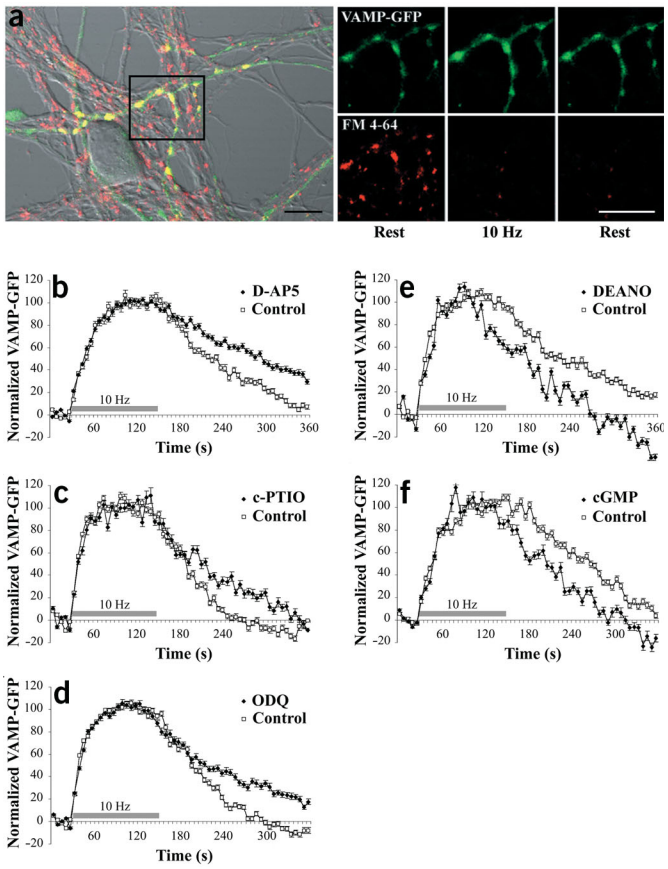

Figure 1 Retrograde regulation of endocytosis. (**a**) Primary cultures of hippocampal neurons were transfected with VAMP–GFP (green) and active presynaptic boutons were identified by loading with FM 4-64 (red). Bouton fluorescence was measured during rest and upon electrical stimulation. Right, a time-lapse sequence of the unloading of the boxed region is shown at a higher magnification, with the two fluorescent channels displayed separately. Scale bar, 10 μm. (**b–f**) Values of VAMP–GFP fluorescence were normalized to the peak of fluorescence change and the pattern of fluorescence decay was compared between control cultures and in the presence of different pharmacological agents (50 μM D-AP5, 30 μM carboxy-PTIO, 10 μM ODQ, 10–50 μM DEANO and 200 μM 8-bromo-cGMP). Mean values of the normalized VAMP–GFP fluorescence intensities and standard errors are shown with $n > 70$ presynaptic boutons from at least four experiments for each condition.

presynaptic boutons have been widely used to quantify clathrin-mediated endocytosis and other aspects of synaptic vesicle recycling[19].

NO can regulate synaptic vesicle endocytosis

Primary cultures of hippocampal neurons, ages 7–15 days *in vitro*, were transfected with VAMP–GFP and loaded with FM 4-64 by electrical stimulation for 30 s at 10 Hz. Transfected axons forming active synapses (*i.e.*, labeled with FM 4-64) were identified for confocal imaging (**Fig. 1a**). Electrical stimulation of the neurons (2 min at 10 Hz) evoked synaptic vesicle exocytosis, and the resulting increase in presynaptic VAMP–GFP fluorescence was on the order of 35%. Fluorescence gradually returned to baseline after the end of stimulation, presumably due to endocytosis and reacidification of vesicles. The time courses of VAMP–GFP intensity changes in presynaptic boutons were compared in control cultures and in the presence of pharmacological agents interfering with the NO retrograde pathway, including an NMDA receptor antagonist (D-AP5), a selective neuronal NOS inhibitor (TRIM, data not shown) and an extracellular NO scavenger (carboxy-PTIO). Each of these agents caused a significant delay in the return to baseline GFP fluorescence (**Fig. 1b,c** and **Table 1**), indicating that interfering with the NMDA-dependent NO retrograde pathway slows synaptic vesicle endocytosis. A major target of NO in brain is the soluble guanylyl cyclase, responsible for the production of cGMP. Application of ODQ, an inhibitor of the NO-sensitive guanylyl cyclase, also slowed synaptic vesicle endocytosis (**Fig. 1d** and **Table 1**), suggesting that NO action is mediated via cGMP.

The average increase in VAMP–GFP fluorescence evoked by 2-min stimulation episodes was not significantly affected by the above pharmacological treatments. Thus, the addition of D-AP5 resulted in an average increase of VAMP–GFP fluorescence of 28 ± 2% (vs. 34 ± 3% for the control). For carboxy-PTIO, this value was 38 ± 4% (vs. 32 ± 3%), and for ODQ, 37 ± 3% (vs. 31 ± 2%). While VAMP–GFP fluorescence intensities reflect the concomitant action of exo- and endo-cytosis during electrical stimulation, this fact reassures us that the observed changes in endocytic rate after the end of stimulation are not due to vastly different numbers of exocytosed synaptic vesicles (see **Supplementary Table 1** online).

If the observed decreases in the rate of synaptic vesicle endocytosis are indeed due to blocking the retrograde NO pathway, then NO donors or cGMP analogs might be expected to speed endocytosis. Application of DEANO and 8-bromo-cGMP to the neuronal cultures did, in fact, result in faster synaptic vesicle endocytosis (**Fig. 1e,f** and **Table 1**). Thus, using a diverse range of agents with both positive and negative effects on NO and cGMP signaling produced results that are consistent with the operation of a pathway analogous to the well-studied cGMP-coupled NO pathway[3].

Higher levels of cGMP correlate with faster endocytosis

The postulated coupling of NO signals via guanylyl cyclase activation and cGMP implies that cGMP levels in boutons should increase when the NO pathway is activated. Indeed, quantitative anti-cGMP immunolabeling of control and stimulated cultures revealed that electrical stimulation causes a massive increase in presynaptic cGMP levels (**Fig. 2a,b**). However, cGMP levels in stimulated cultures varied greatly from bouton to bouton (**Fig. 2c–e**). Given such variability, one might expect that boutons showing the largest cGMP elevations might also show the largest effects on endocytosis. We therefore examined the relationship between the amount of cGMP produced in individual presynaptic boutons and the speed of endocytosis at that bouton. VAMP–GFP was used to monitor endocytosis after electrical stimulation. After a brief rest, the neurons were stimulated again and immediately fixed. The amount of cGMP produced within individual boutons was determined by retrospective immunostaining. Boutons with high levels of cGMP showed a faster rate of endocytosis than did boutons with low levels of cGMP in the same neuronal cultures (**Fig. 2f**), strongly supporting the idea that cGMP is involved in regulating the rate of endocytosis. This experimental design was based on the assumption that synaptic vesicle recycling in individual boutons follows a similar pattern in consecutive rounds of stimulation. We confirmed this by comparing VAMP–GFP signals during two consecutive rounds of stimulation: the time constants of fluorescence decay of individual boutons were positively correlated with a correlation coefficient of 0.72 ($P < 0.001$; $n = 41$ from three experiments).

PIP2 involvement in the regulation of endocytosis

These experiments suggest a previously unknown function for the NO retrograde pathway: regulation of synaptic vesicle endocytosis.

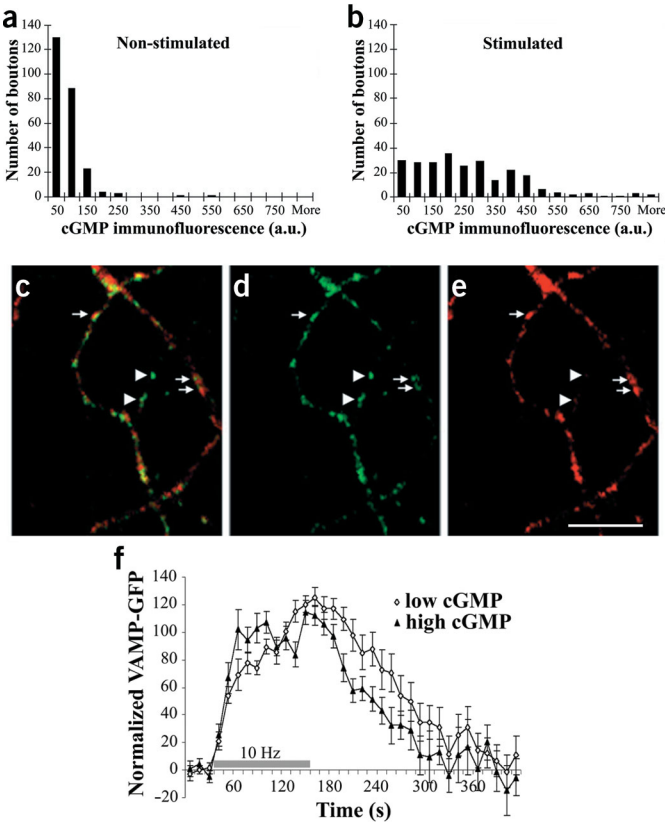

Figure 2 Cyclic GMP production within presynaptic boutons upon electrical stimulation. (**a–e**) Neuronal cultures were stimulated for 2 min at 10 Hz and immediately fixed. They were then processed for immunolabeling of synapsin (green) and cGMP (red). (**a**,**b**) Electrical stimulation caused an overall massive increase in cGMP immunostaining (arbitrary units) compared to nonstimulated cultures. (**c–e**) The cGMP content of individual boutons, however, varied greatly, with some remaining at pre-stimulation levels (arrowheads), while others showed very substantial increase (arrows). Scale bar, 10 μm. (**f**) Presynaptic cGMP levels correlate with the rate of endocytosis. VAMP–GFP was used to monitor endocytosis following electrical stimulation. After a brief rest, the neurons were stimulated again, then fixed immediately and processed for cGMP immunocytochemistry. For each experiment, boutons were assigned to one of three categories (low, medium and high cGMP content) according to their ratio of cGMP to VAMP–GFP fluorescence, with each category containing an equal number of boutons. Changes in VAMP–GFP fluorescence were compared between boutons with low and high levels of cGMP produced in response to electrical stimulation ($n = 24$ and $n = 23$, respectively, from two separate experiments).

This NO action is mediated via activation of guanylyl cyclase and the production of cGMP. A candidate downstream effector in this pathway is PIP2; we have previously shown that retrograde NO signaling modulates the availability of this lipid[8]. To investigate the potential involvement of presynaptic PIP2 in the NO retrograde regulation of endocytosis, we tested for effects of two different experimental reductions in PIP2 availability on the rate of endocytosis. First, the time courses of VAMP–GFP intensity changes in presynaptic boutons were compared in control cultures and in the presence of PAO, a drug shown to reduce levels of PIP2[20,21]. PAO is an inhibitor of PI 4-kinase, which is involved in the production of PIP, the precursor for PIP2. The addition of PAO mimicked the effects of inhibitors of the NO retrograde pathway (**Fig. 3a**). After electrical stimulation in the presence of PAO, VAMP–GFP fluorescence recovered with a time constant of 156.2 ± 15.6 s ($n = 4$ experiments with a total of 112 boutons), compared to the control time constant of 76.2 ± 16.9 s ($n = 6$ experiments with a total of 149 boutons; $P < 0.05$, Wilcoxon nonparametric test).

To check for potential nonspecific effects of PAO and to test independently for a role of PIP2 in synaptic vesicle endocytosis, we next used the phospholipase C δ1 pleckstrin homology (PH) domain fused to GFP. This PH domain binds specifically and with high affinity to PIP2 (ref. 22). At low levels of expression, it can be used to monitor PIP2 distribution[8], whereas at higher expression levels it can interfere with PIP2 function by substantially reducing its availability[21]. Hippocampal cultures were transfected with PH–GFP and the function of presynaptic boutons was assessed using the fluorescent dye FM 4-64. To measure the rate of endocytosis, we assessed the effects of adding the dye with a certain delay after the beginning of electrical stimulation[23]. With this procedure, some vesicles undergo endocytosis before addition of the dye and thus remain unstained. The more slowly endocytosis proceeds, the fewer vesicles will escape labeling and the higher will be the intensity of FM 4-64 staining of the synapse. In such experiments, the FM 4-64 labeling of transfected synapses was invariably higher than the labeling of control synapses (78.2 ± 3.7% for transfected synapses, compared to 63.2 ± 2.2% for control synapses, $P < 0.001$, t-test; **Fig. 3b**). This strongly indicates that endocytosis proceeds more slowly when the availability of PIP2 is reduced by binding to PH–GFP. Thus, both types of experiment provide strong evidence that presynaptic PIP2 can regulate the speed of synaptic vesicle endocytosis.

Table 1 Time constants of recovery of VAMP–GFP fluorescence after electrical stimulation (2 min at 10 Hz)

	mean ± s.e.m.	n	P-value
Control	83.7 ± 14.2	8	< 0.05
D-AP5	179.6 ± 42.8	5	
Control	53.3 ± 9.4	6	< 0.05
carboxyPTIO	115.2 ± 29.6	7	
Control	59.0 ± 9.5	6	< 0.01
ODQ	154.0 ± 28.7	4	
Control	123.9 ± 15.2	8	< 0.05
DEANO	78.9 ± 9.6	7	
Control	166.9 ± 15.2	6	< 0.01
cGMP	69.4 ± 19.2	6	

Time constants were obtained by fitting fluorescence decays from individual experiments with a single exponential. The Wilcoxon nonparametric test was used for the statistical analysis. Because of variability between neuronal culture preparations, all experimental groups were compared with controls from the same neuronal preparation done on the same day.

PIP2 and synaptic vesicle exocytosis

Because PIP2 has been implicated in synaptic vesicle exocytosis[9–11], we conducted experiments to evaluate possible PIP2 effects on exocytosis under our experimental conditions. Hippocampal neurons were transfected with PH–GFP, loaded with FM 4-64 and imaged at rest and during subsequent unloading. The initial FM 4-64 loading, which is proportional to the number of recycled vesicles, was the same for PH–GFP transfected and nontransfected synapses (659 ± 83 versus 630 ± 100 arbitrary units (a.u.), respectively, $n = 15$ experiments with 339 transfected and 714 control synapses). This suggests that the number of vesicles exocytosed is not affected by

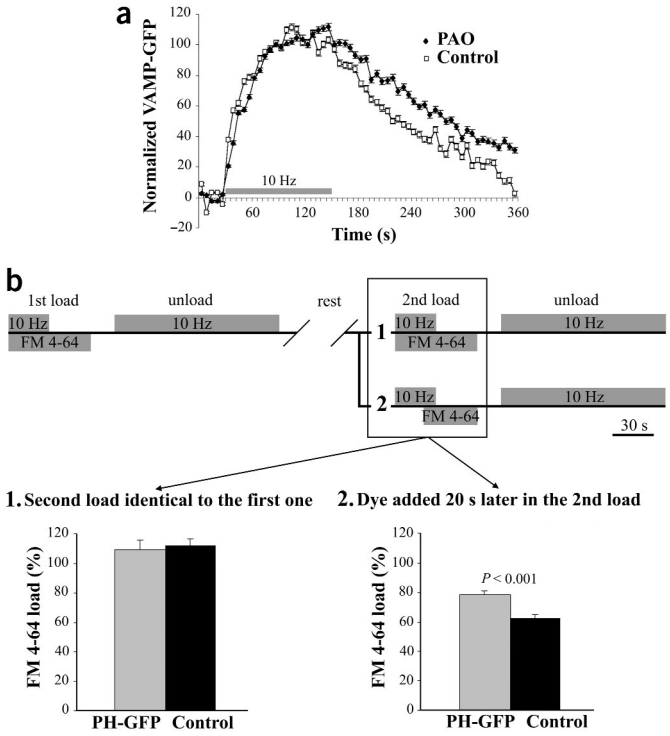

Figure 3 Reduction of PIP2 availability results in slower endocytosis. (**a**) We carried out experiments similar to those shown in **Fig. 1b–f** to compare endocytosis in neuronal cultures treated with PAO (1 μM) to that in control cultures. (**b**) Sequestering PIP2 with PH–GFP also resulted in a defect in synaptic vesicle endocytosis. Neurons were transfected with PH–GFP and two consecutive load-unload cycles with FM 4-64 were performed. FM 4-64 loading intensities were expressed as percentage of the intensity of the first load and averaged across the synaptic population. For control condition 1, there were 56 boutons transfected with PH–GFP and 167 nontransfected boutons from four experiments. For condition 2, $n = 37$ PH–GFP and 123 nontransfected boutons from three experiments.

PIP2 scavenging under these conditions. The rate of synaptic vesicle exocytosis (measured as the rate of unloading of the releasable dye) was also essentially the same (**Fig. 4a**). It should be noted that very high levels of PH–GFP expression slowed down the rate of exocytosis (not shown), but neurons showing such high expression levels were excluded from the experimental analyses presented here. Thus, the effects of PIP2 on endocytosis reported here are very unlikely to be secondary to effects on exocytosis.

PIP2 may also regulate post-endocytic steps in vesicle recycling

Although synaptic vesicle exocytosis was apparently unaffected by moderate levels of PH–GFP expression, transfected synapses retained a significantly higher fraction of residual FM 4-64. This is evident when the data from **Fig. 4a** are presented as unloading curves normalized to the initial resting state of FM 4-64 fluorescence (**Fig. 4b**). Thus, 1 min after the end of a 2-min stimulation of 10 Hz, transfected synapses had retained 50% more dye (0.30 ± 0.01 of the initial FM 4-64 fluorescence vs. 0.20 ± 0.01 for control; $P < 0.001$, t-test; $n = 339$ transfected and 714 control synapses from 15 experiments). The difference between the fractions of residual dye in transfected and control synapses was 0.1 ± 0.01 (**Fig. 4c**). A similar difference in residual fluorescence was achieved when using PAO to reduce PIP2 levels (0.1 ± 0.01 more than control, $P < 0.001$, t-test, $n = 57$ from four experiments for PAO and $n = 105$ from three experiments for control). Because, as indicated in the previous paragraph, there was no other indication for a defect in exocytosis from our experiments (**Supplementary Fig. 1** online), the increase in residual fluorescence most probably reflects a change in the recycling of dye-loaded vesicles. The simplest possibility would be a slowing in the rate at which recently loaded and endocytosed vesicles become competent for a second round of stimulated release and unloading. We have tested this possibility by measuring the fraction of dye retained by transfected and control synapses as a function of varied intervals between loading and unloading stimuli (**Fig. 4c**). When 10 min had elapsed between the loading and unloading stimulation, transfected synapses retained 0.12 ± 0.03 more dye, on average, than control synapses, and this difference increased to 0.25 ± 0.04 at 5 min ($P < 0.01$, t-test; $n = 52$ transfected and 117 control synapses from three experiments). Thus, PIP2 availability seems to regulate not only synaptic vesicle endocytosis, but also at least one step in recycling subsequent to the completion of the dye-loading endocytosis.

PIP2 as an effector in the NO retrograde pathway

If PIP2 is indeed part of the NO retrograde pathway regulating synaptic vesicle endocytosis and subsequent recycling, then the effect of reducing PIP2 availability and blocking the initial steps of this pathway should be occlusive rather than additive. To test this hypothesis, we loaded presynaptic boutons with FM 4-64 and

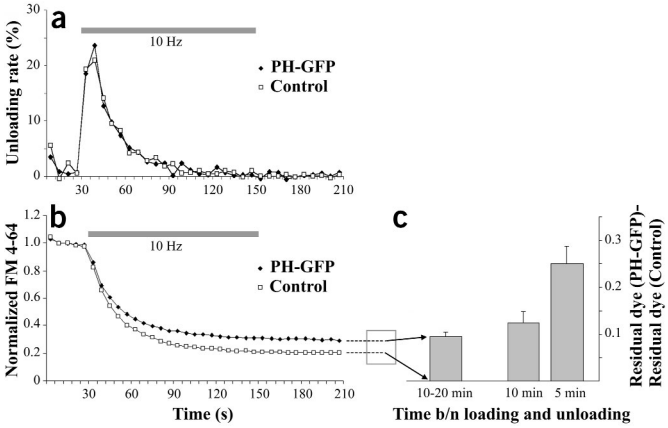

Figure 4 Effect of scavenging PIP2 by PH–GFP on FM 4-64 unloading. (**a**) Reducing PIP2 availability by overexpression of PH–GFP does not significantly affect the rate of unloading of the releasable FM 4-64. Unloading rates are fluorescence differences between successive time points expressed as percentages of total releasable fluorescence. Neurons were loaded by an electrical stimulation of 10 Hz for 30 s in the presence of FM 4-64, and after an additional 30 s, the dye was washed away. FM unloading was achieved by 10-Hz stimulation for 2 min ($n = 339$ transfected and 714 control synapses from 15 experiments). (**b**) Same data, presented as unloading curves with FM 4-64 fluorescence intensities normalized to the initial resting state of each presynaptic bouton. (**c**) Difference in the unloading of transfected and control synapses in relation to the time elapsed between loading and unloading. The 10–20 min bar is from the same experiment as **a** and **b**. For the 10-min and 5-min bars, $n = 52$ transfected and 117 control synapses from three experiments. Standard errors are not presented in **a** and **b** because they were on the order of 1% in **a** and 0.01% in **b**.

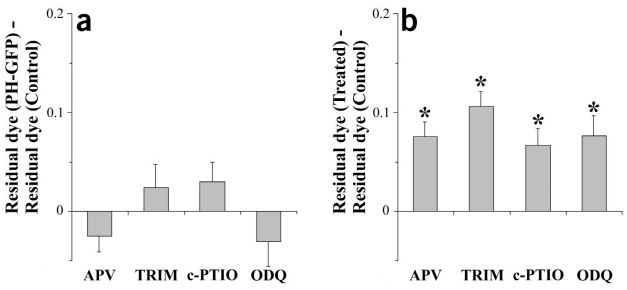

Figure 5 The effects of reducing PIP2 availability and blocking NO signaling are not additive. (**a**) The difference in residual FM 4-64 staining (average of last five time points at the end of a 2-min stimulation of 10 Hz) between PH–GFP and nontransfected synapses in the presence of APV (50 μM), TRIM (100 μM), carboxy-PTIO (30 μM) or ODQ (10 μM). (**b**) Using nontransfected cultures, the difference in residual FM 4-64 staining was compared between pharmacologically treated and control synapses. Standard errors shown. *$P < 0.001$. For each experimental condition, data are from a series of at least three independent experiments with $n > 50$.

imaged at rest and during subsequent unloading. As described above, slowing of synaptic vesicle recycling by reducing available PIP2 resulted in significantly higher residual fluorescence, most probably because it took longer for synaptic vesicles to become available for a second round of stimulated unloading. The addition of drugs blocking the retrograde NO pathway (D-AP5, TRIM, carboxy-PTIO and ODQ) abolished the difference that was previously observed between the unloading of PH–GFP transfected and control synapses (compare **Figs. 5a** and **4c**). Thus, while the drugs affected non-transfected synapses (**Fig. 5b**), they did not have any additional effect on PH–GFP transfected synapses. These experiments provide further evidence for PIP2 mediation of the retrograde NO effect on synaptic vesicle recycling.

The NO pathway during sustained neurotransmitter release

By augmenting the speed of synaptic vesicle endocytosis and subsequent recycling, the retrograde pathway proposed here might be expected to enhance sustained neurotransmitter release during prolonged stimulation. Indeed, when nontransfected synaptic boutons were tested twice serially with the same FM 4-64 protocol (30 s at 10 Hz load; 2 min at 10 Hz unload), they took up equal amounts of the dye, even when the second loading session closely followed the first (90 s). In contrast, PH–GFP transfected synapses loaded at a significantly lower level the second time (79.7 ± 5.6% of first load versus 106.3 ± 6.6% for nontransfected synapses, $P = 0.01$, t-test, $n = 41$ PH–GFP synapses and 92 nontransfected synapses from two experiments). Nevertheless, when the time between the two loading sessions was increased (7–10 min), PH–GFP synapses behaved similarly to the nontransfected synapses and loaded equally well both times (**Fig. 3b**, condition 1). This suggests that the NO retrograde pathway and presynaptic PIP2 regulation may have a major impact on synaptic function under conditions of relatively intense and sustained synaptic transmission.

Ultrastructural localization of PH–GFP

How might PIP2 mediate the retrograde modulation of synaptic vesicle endocytosis and later steps of recycling? To address this question, we examined the ultrastructural distribution of PH–GFP in order to localize sites at which it may interfere with PIP2 action. PH–GFP was found mainly on the cytoplasmic membrane of resting neurons, where PIP2 is known to be localized[24,25] (**Fig. 6a,b,e**). In electrically stimulated synapses, on the other hand, PH–GFP was concentrated within the synapse, often in association with vesicles of various sizes (**Fig. 6c,e**). PH–GFP was also seen immediately adjacent to microtubules (in 9 of 87 presynaptic boutons), membrane invaginations (3 of 87, **Fig. 6d**) or tubular structures (2 of 87). Meanwhile, in other neuronal compartments, for example dendritic shafts or spines (**Fig. 6e**), PH–GFP distribution did not change upon electrical stimulation. The ultrastructural localization of PH–GFP and its changes with stimulation thus suggest a fairly direct action of PIP2 on recycling synaptic membranes.

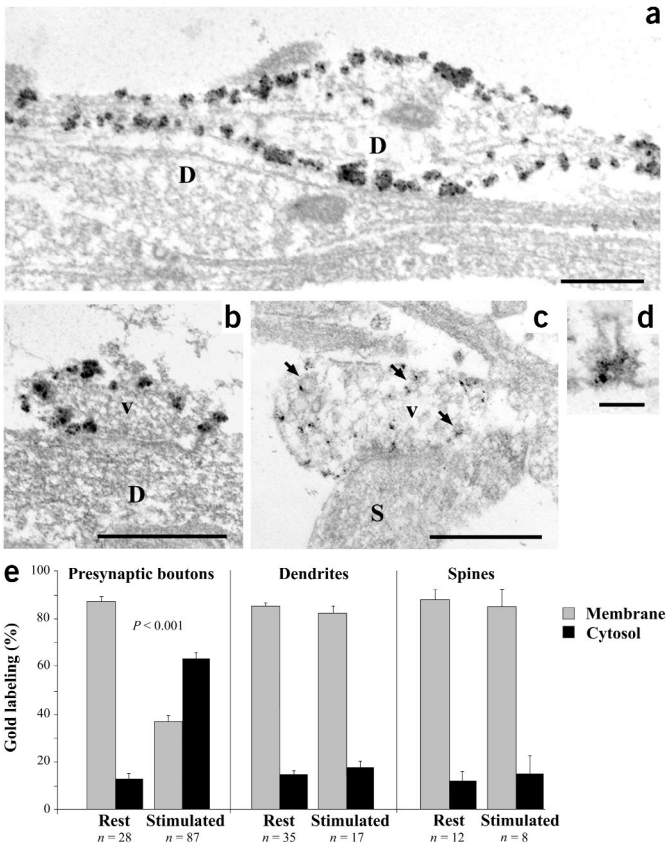

Figure 6 ImmunoEM of hippocampal neuronal cultures showing the ultrastructural distribution of PH–GFP as detected with a monoclonal antibody against GFP. (**a**,**b**) PH–GFP has a predominantly plasma membrane localization in resting neurons, as shown on dendrites (**a**) and presynaptic boutons (**b**). (**c**,**d**) At the end of electrical stimulation (2 min at 10 Hz), PH–GFP is found concentrated within the cytoplasm of presynaptic boutons, often in association with vesicles of various sizes (arrows in **c**) and sometimes at membrane invaginations (**d**). In stimulated neurons, a shorter silver intensification was used to avoid obscuring the precise localization of the signal. D, dendrite; v, synaptic vesicles; S, dendritic spine. Scale bars, 0.5 μm (**a–c**) and 0.1 μm (**d**). (**e**) Quantitative distribution of the immunolabel at rest and after stimulation. After stimulation, there is a statistically significant change ($P < 0.0001$, t-test) in the immunolabel distribution in presynaptic boutons, but not in dendritic shafts or spines. Standard errors are shown.

DISCUSSION

The present experiments provide evidence for the existence of a retrograde pathway for regulating synaptic vesicle endocytosis and later stages of recycling. This retrograde pathway requires activation of postsynaptic NMDA receptors, production of NO and its diffusion to the presynaptic side, leading ultimately to an increase in presynaptic PIP2.

Dissecting the synaptic vesicle cycle

During neuronal activity, synaptic vesicles function in a cycle: they undergo exocytosis, followed by endocytosis, postendocytic processing and repriming, then exocytosis again. Promoting or interfering with this cycle at any one stage may sooner or later affect all stages. It is well known from the literature that NO can induce or modulate neurotransmitter release[3–7], and a variety of mechanisms for such actions have been proposed. In the present study, however, we have focused on direct effects of the NO retrograde pathway on endocytosis and subsequent recycling of synaptic vesicles. We have shown that activation of this pathway increases rates of endocytosis and some subsequent recycling step, and that it can do so under conditions where no consistent effect on exocytosis is observable. It is thus very unlikely that either of the recycling effects we have documented are secondary to some more direct effect on exocytosis. Nonetheless, we have also shown that direct effects on endocytosis and recycling can ultimately modulate action potential–induced synaptic vesicle exocytosis, a modulation which becomes particularly prominent under conditions of sustained neurotransmission. Such modulation does not seem surprising given the cyclic nature of vesicle function.

PIP2 as a regulator of synaptic vesicle recycling

PIP2 has been extensively implicated in the process of endocytosis[9–11]. Until now, however, there has been no direct demonstration of the functional effects of modifying PIP2 availability on the synaptic vesicle cycle in intact synapses. The present experiments reveal that limiting PIP2 availability can significantly reduce the rates of synaptic vesicle endocytosis and recycling. The PIP2 modulation of the vesicle cycle appears to occur at more than one stage: endocytosis proper and at least one later step of recycling. The FM 4-64 experiment, in which we introduced dye with a certain delay after the beginning of stimulation (**Fig. 3b**), indicates a PIP2 involvement in the endocytosis of synaptic vesicles, in particular the formation and/or closing off of the clathrin-coated pits. The VAMP–GFP data give further support to a role in the initial stages of synaptic vesicles recycling (closing off and acidification of newly formed endocytic vesicles). In addition, comparisons of the residual FM staining after unloading indicate a PIP2 involvement at subsequent stages of endocytosis and synaptic vesicle maturation, perhaps involving clathrin uncoating, endocytic vesicle trafficking or some other vesicle repriming step.

The specific localization of PH–GFP at the ultrastructural level and its characteristic changes during electrical stimulation are also in agreement with a direct involvement of PIP2 at several steps of synaptic vesicle recycling. The presence of PH–GFP on the plasma membrane in resting cells and on plasma membrane invaginations in stimulated cells is consistent with a direct PIP2 action at early stages of endocytosis, such as formation and/or closing off of clathrin-coated pits. The localization of PH–GFP within the stimulated synapse, and in particular on synaptic vesicles and other vesicular structures, also suggests PIP2 involvement at later stages of endocytosis and synaptic vesicle maturation. Thus, it is unlikely that the functional effects we found are indirectly due to changes in Ca^{2+} concentration[17,26,27], which may result from changes in IP3 levels[28] or through a PIP2 regulation of voltage-gated Ca^{2+} channels[29]. Our conclusions are consistent with previous studies, using mainly *in vitro* biochemical approaches, which suggest direct PIP2 involvement in multiple steps of synaptic vesicle recycling. These include the formation of clathrin-coated pits via the PIP2 interaction with AP180, epsin and AP2[30–32], the pinching off of endocytic vesicles via PIP2 interaction with dynamin[33,34], the uncoating of endocytosed vesicles requiring hydrolysis of PIP2 by synaptojanin[35] and the transport of endocytic vesicles because of the PIP2-dependence of actin assembly[36].

Activity-dependent regulation of endocytosis and recycling

Our present results indicate that PIP2 regulation of synaptic vesicle endocytosis and subsequent recycling is part of an activity-dependent retrograde pathway. This pathway comprises postsynaptic NMDAR activation, the production of NO, and its retrograde diffusion to presynaptic sites where it increases PIP2 via a cGMP-dependent mechanism. The retrograde nature of the NO effect on presynaptic PIP2 was explored in more detail in a previous study[8], where we used immunofluorescence to show the postsynaptic distribution of NMDA receptors in hippocampal cultures. This is in agreement with recent data from intact hippocampus showing that the NR2 subunit of the NMDA receptor and NOS-I are concentrated in postsynaptic densities, whereas soluble guanylyl cyclase is concentrated presynaptically[14]. There is also functional evidence for the retrograde action of NO in cultured hippocampal neurons[4].

The mechanism by which NO can lead to an increase in PIP2 at the synapse is still not known. Theoretically, this might be achieved either by stimulating its synthesis or inhibiting its chemical transformation. Thus, likely targets of NO action would include enzymes involved in the synthesis of PIP2, such as PIP kinase Iγ, the major PIP2 synthesizing enzyme at the synapse[37], and PI 4-kinase IIα, responsible for the generation of PI(4)P[38], the precursor of PIP2. On the other hand, NO may be acting through enzymes involved in the hydrolysis of PIP2, for example PLC, which hydrolyses PIP2 to IP3 and diacylglycerol, or synaptojanin, which dephosphorylates PIP2 (ref. 39). A study in non-neuronal cells suggests that NO can negatively modulate PIP2 hydrolysis through the action of a cGMP-dependent protein kinase I on PLC[40].

As we have shown in the present study, the NO-dependent retrograde pathway can have an important impact on synaptic function, for example, by modulating synaptic vesicle recycling in such a way as to help sustain high levels of neurotransmitter release. In addition, the existence of such a pathway suggests a range of new possibilities for the modulation of synaptic function that would not have been envisioned from previous models of the regulation of endocytosis. Because NMDAR activation is required for generation of the NO signal, regulation of endocytosis becomes contingent not only on the function of the individual presynaptic bouton, but also on postsynaptic events reflecting much broader integration of local network activity. This is true by virtue of the well-known voltage dependence of NMDAR activation and thus on the aggregate of all excitatory and inhibitory inputs to a given neuron. In addition, because NO may diffuse from nearby synapses, endocytosis at a given bouton also may be regulated by cells other than the immediate postsynaptic partner. The discovery of retrograde regulation of synaptic endocytosis and recycling may thus substantially advance our understanding of the function of both individual synapses and the neuronal networks in which they are embedded.

METHODS

Cell culture and transfection. Primary embryonic hippocampal cultures were prepared and used 7–15 d later. We used the 'Banker style' cultures[41] of pure neurons to exclude possible effects of glia. All procedures were approved by the Institutional Animal Care and Use Committee of Stanford University. Neurons were transfected with VAMP–GFP (gift from R. Scheller, Genetech Inc.) or PH–GFP (gift from T. Balla, NIH) using a modified calcium phosphate transfection protocol[42]. Neurons with very high levels of VAMP–GFP or PH–GFP expression were excluded from analysis. Very high levels of expression were defined as those having a fluorescence intensity of at least twice the average level for each series of experiments (*i.e.*, experiments from the same neuronal preparation performed on the same day).

Confocal microscopy of live neurons and image analysis. During imaging, neurons were kept at 37 °C in Tyrode's solution (119 mM NaCl, 2.5 mM KCl, 2 mM $CaCl_2$, 2 mM $MgCl_2$, 25 mM HEPES, pH 7.4) with the addition of 30 mM glucose, 1% ovalbumin and 10 μM 6-cyano-7-nitroquinoxaline-2,3-dione (CNQX, an AMPA/kainate receptor antagonist used to block spontaneous recurrent excitatory activity). FM 4-64 loading was performed by superfusing the dye (5 μM) into the imaging chamber and electrically stimulating the neurons by passing current pulses between platinum electrodes placed at opposite ends of the chamber. Stimulation of 10 Hz for 30 s was applied, and after an additional 30 s, the dye was washed away. FM unloading was achieved by electrical stimulation of 10 Hz for 2 min. This loading protocol labels approximately 75% of the synaptic vesicle pool and the unloading stimulation ensures that essentially all the pool is used[23].

Imaging was done with a scanning laser confocal microscope designed by S.J.S. using a Zeiss 40×/1.3 NA Fluar objective. Images were sampled at 0.286 μm pixel size and collected every 6 s. Images were analyzed with custom software (N.E. Ziv, Technion). FM 4-64 or PH–GFP fluorescence intensities were averaged over 6×6 pixel squares centered on presynaptic boutons. When analyzing VAMP–GFP transfected neurons, VAMP–GFP fluorescence intensities were averaged over entire presynaptic boutons and immediately adjacent regions.

Pharmacology. The following reagents were used: D(-)-2-amino-5-phosphonopentanoic acid (50 μM in 50 μM NaOH; Tocris), TRIM (100 μM in 0.1% DMSO; Molecular Probes), carboxy-PTIO (30 μM; Molecular Probes), ODQ (10 μM in 0.01% DMSO; Tocris), DEANO (10–50 μM in 2–10 μM NaON; Molecular Probes), 8-bromo-cGMP (200 μM; Tocris), PAO (1 μM in 0.05% DMSO; Sigma Aldrich). In most cases, stock solutions (1,000–10,000×) were added directly to the Tyrode's solution immediately before the experiment and neurons were incubated for 5 min before loading with FM 4-64. DEANO and 8-bromo-cGMP were added to the Tyrode's solution after loading with FM 4-64, and unloading began 2 min after addition of the drugs.

Immunostaining. Cells were fixed in 4% formaldehyde and 4% sucrose in PBS at 37 °C for 20 min, permeabilized in 0.3% Triton for 5 min, blocked in 5% bovine serum albumin (BSA) and 5 % normal goat serum (NGS) in PBS at 37 °C for 1 h, then incubated in primary antibody (anti-cGMP, rabbit, Chemicon, 1:300, or anti-synapsin, mouse, Chemicon, 1:1,000 in PBS with 1% NGS) for 2 h and finally secondary antibody (goat anti-rabbit CY-5, Jackson Immuoresearch, 1:800, or goat anti-mouse Alexa 488, Molecular Probes, 1:2,000) for 30 min. All the steps excluding fixation and blocking were performed at room temperature.

Immuno-electron microscopy (immunoEM). Hippocampal neuronal cultures transfected with PH–GFP were fixed in 1% glutaraldehyde and 4% formaldehyde in PBS using rapid microwave irradiation (PELCO 3451 laboratory microwave system; Ted Pella; one cycle of 20 s on—20 s off—20 s on at 100 W, and two cycles at 450 W) and ColdSpot (Ted Pella) set at 5 °C. After rinsing in PBS, the cells were quenched in 50 mM glycine in PBS (2× for 1 min in the microwave at 100 W), rinsed again, permeabilized with 0.1% saponin in PBS for 1 min at room temperature, rinsed and blocked in a solution of NGS (1%), BSA (1%) and fish gelatin (0.1%) in PBS (one cycle of 1 min on—1 min off—1 min on at 250 W). The cells were rinsed in PBS-BSA (0.1 % BSA, 0.1 % fish gelatin and 0.05 % Tween in PBS), then incubated in primary antibody (anti-GFP, mouse, Boehringer Mannheim, 1:200 in PBS-BSA with 1% NGS; one cycle of 2 min on—2 min off—2 min on at 250 W), rinsed well in PBS-BSA and incubated in secondary antibody (Nanogold, Nanoprobes, 1:40 in PBS-BSA, one cycle of 2 min on—2 min off—2 min on at 250 W). The Nanogold was silver intensified with HQ Silver (Nanoprobes). Finally, the neurons were postfixed with osmium tetroxide (0.1%) and potassium ferricyanide (0.8%) in cacodylate buffer (one cycle of 20 s on—20 s off—20 s on at 100 W, then 5 min at room temperature), dehydrated in ascending ethanol series (30 s at 350 W each in 50%, 70%, 95% and three times in 100%) and infiltrated in Embed 812 (EMS; 5 min at 350 W each in 1 part resin/1 part ethanol, 2 parts resin/1 part ethanol, and pure resin), then flat-embedded overnight at 60 °C. Glass coverslips were dissolved in hydrofluoric acid for 15 min. Ultrathin sections were cut with an ultramicrotome (Ultracut E, Reichert-Jung), post-stained with uranyl acetate and lead citrate and viewed with a JEM-1230 electron microscope (JEOL) at 80 kV accelerated voltage using a Gatan 791 CCD camera.

Note: Supplementary information is available on the Nature Neuroscience website.

ACKNOWLEDGMENTS

We thank R.W. Aldrich and the members of the Smith lab for critical reading of the manuscript and Y. Gedde for technical assistance. This work was supported by grants from the US National Institutes of Health and a gift from the Vincent Coates Foundation.

COMPETING INTERESTS STATEMENT

The authors declare that they have no competing financial interests.

Received 29 April; accepted 23 June 2003
Published online at http://www.nature.com/natureneuroscience/

1. Tao, H.W. & Poo, M. Retrograde signaling at central synapses. *Proc. Natl. Acad. Sci. USA* **98**, 11009–11015 (2001).
2. Wilson, R.I. & Nicoll, R.A. Endocannabinoid signaling in the brain. *Science* **296**, 678–682 (2002).
3. Prast, H. & Philippu, A. Nitric oxide as modulator of neuronal function. *Prog. Neurobiol.* **64**, 51–68 (2001).
4. Arancio, O., Kandel, E.R. & Hawkins, R.D. Activity-dependent long-term enhancement of transmitter release by presynaptic 3′,5′-cGMP in cultured hippocampal neurons. *Nature* **376**, 74–80 (1995).
5. Meffert, M.K., Calakos, N.C., Scheller, R.H. & Schulman, H. Nitric oxide modulates synaptic vesicle docking/fusion reactions. *Neuron* **16**, 1229–1236 (1996).
6. Sporns, O. & Jenkinson, S. Potassium ion- and nitric oxide-induced exocytosis from populations of hippocampal synapses during synaptic maturation *in vitro*. *Neuroscience* **80**, 1057–1073 (1997).
7. Klyachko, V.A., Ahern, G.P. & Jackson, M.B. cGMP-mediated facilitation in nerve terminals by enhancement of the spike after hyperpolarization. *Neuron* **31**, 1015–1025 (2001).
8. Micheva, K.D., Holz, R.W. & Smith, S.J. Regulation of presynaptic phosphatidylinositol 4,5-biphosphate by neuronal activity. *J. Cell Biol.* **154**, 355–368 (2001).
9. Cremona, O. & De Camilli, P. Phosphoinositides in membrane traffic at the synapse. *J. Cell Sci.* **114**, 1041–1052 (2001).
10. Martin, T.F.J. PI(4,5)P(2) regulation of surface membrane traffic. *Curr. Opin. Cell Biol.* **13**, 493–499 (2001).
11. Osborne, S.L., Meunier, F.A. & Schiavo, G. Phosphoinositides as key regulators of synaptic function. *Neuron* **32**, 9–12 (2001).
12. Rao, A., Kim, E., Sheng, M. & Craig, A.-M. Heterogeneity in the molecular composition of excitatory postsynaptic sites during development of hippocampal neurons in culture. *J. Neurosci.* **18**, 1217–1229 (1998).
13. Wendland, B. *et al.* Existence of nitric oxide synthase in rat hippocampal pyramidal cells. *Proc. Natl. Acad. Sci. USA* **91**, 2151–2155 (1994).
14. Burette, A., Zabel, U., Weinberg, R. J., Schmidt, H.H.H.W. & Valtschanoff, J.G. Synaptic localization of nitric oxide synthase and soluble guanylyl cyclase in the hippocampus. *J. Neurosci.* **22**, 8961–8970 (2002).
15. Son, H. *et al.* Long-term potentiation is reduced in mice that are doubly mutant in endothelial and neuronal nitric oxide synthase. *Cell* **87**, 1015–1023 (1996).
16. De Camilli, P., Slepnev, V.I., Shupliakov, O. & Brodin, L. Synaptic vesicle endocytosis. in *Synapses* (eds. Cowan, M.W., Sudhof, T.C. & Stevens, C.F.) 217–274 (The Johns Hopkins Univ. Press, Baltimore, MD, 2001).
17. Li, Z. & Murthy, V.N. Visualizing postendocytic traffic of synaptic vesicles at hippocampal synapses. *Neuron* **31**, 593–605 (2001).
18. Betz, W.J., Mao, F. & Bewick, G.S. Activity-dependent fluorescent staining and destaining of living motor nerve terminals. *J. Neurosci.* **12**, 363–375 (1992).
19. Ryan, T.A. Presynaptic imaging techniques. *Curr. Opin. Neurobiol.* **11**, 544–549 (2001).
20. Khvotchev, M. & Südhof, T. Newly synthesized phosphatidylinositol phosphates

are required for synaptic norepinephrine but not glutamate or γ-aminobutyric acid (GABA) release. *J. Biol. Chem.* **273**, 21451–21454 (1998).
21. Varnai, P. & Balla, T. Visualization of phosphoinositides that bind pleckstrin homology domains: calcium- and agonist-induced dynamic changes and relationship to myo-[^{3}H]inositol-labeled phosphoinositide pools. *J. Cell Biol.* **143**, 501–510 (1998).
22. Paterson, H.F. *et al.* Phospholipase C delta 1 requires a pleckstrin homology domain for interaction with the plasma membrane. *Biochem. J.* **312**, 661–666 (1995).
23. Ryan, T.A. & Smith, S.J. Vesicle pool mobilization during action potential firing at hippocampal synapses. *Neuron* **14**, 983–989 (1995).
24. Hokin, L. & Hokin, M.R. *Biochim. Biophys. Acta* **84**, 563–575 (1964).
25. Eichberg, J. & Dawson, R.M. Polyphosphoinositides in myelin. *Biochem. J.* **96**, 644–650 (1965).
26. Klingauf, J., Kavalali, E.T. & Tsien, R.W. Kinetics and regulation of fast endocytosis at hippocampal synapses. *Nature* **394**, 581–585 (1998).
27. Sankaranarayanan, S. & Ryan, T.A. Calcium accelerates endocytosis of vSNAREs at hippocampal synapses. *Nat. Neurosci.* **4**, 129–136 (2001).
28. Berridge, M.J., Lipp, P. & Bootman, M.D. The versatility and universatility of calcium signalling. *Nat. Rev. Mol. Cell Biol.* **1**, 11–21 (2000).
29. Wu, L., Bauer, C.S., Zhen, X., Xie, C. & Yang, J. Dual regulation of voltage-gated calcium channels by PtdIns(4,5)P2. *Nature* **419**, 947– 952 (2002).
30. Gaidarov, I. & Keen, J.H. Phosphoinositide-AP-2 interactions required for targeting to plasma membrane clathrin-coated pits. *J. Cell Biol.* **146**, 755–764 (1999).
31. Ford, M.G.J. *et al.* Simultaneous binding of PtdIns(4,5)P2 and clathrin by AP180 in the nucleation of clathrin lattices on membranes. *Science* **291**, 1051–1055 (2001).
32. Itoh, T. *et al.* Role of the ENTH domain in phosphatidylinositol-4,5,-biphosphate binding and endocytosis. *Science* **291**, 1047–1051 (2001).
33. Lin, H.C. & Gilman, A.G. Regulation of dynamin I GTPase activity by G protein beta gamma subunits and phosphatidylinositol 4,5-biphosphate. *J. Biol. Chem.* **271**, 27979–27982 (1996).
34. Zheng, J. *et al.* Identification of the binding site for acidic phospholipids on the PH domain of dynamin: Implications for stimulation of GTPase activity. *J. Mol. Biol.* **255**, 14–21 (1996).
35. Cremona, O. *et al.* Essential role of phosphoinositide metabolism in synaptic vesicle recycling. *Cell* **99**, 179–188 (1999).
36. Rozelle, A.L. *et al.* Phosphatidylinositol 4,5-biphosphate induces actin-based movement of raft-enriched vesicles through WASP-Arp2/3. *Curr. Biol.* **10**, 311–320 (2000).
37. Wenk, M.R. *et al.* PIP kinase Iγ is the major PI(4,5)P2 synthesizing enzyme at the synapse. *Neuron* **32**, 79–88 (2001).
38. Guo, J. *et al.* Phosphatidylinositol 4-kinase type IIα is responsible for the phosphatidylinositol 4-kinase activity associated with synaptic vesicles. *Proc. Natl. Acad. Sci. USA* **100**, 3995–4000 (2003).
39. McPherson, P.S. *et al.* A presynaptic inositol-5-phosphatase. *Nature* **379**, 353–357 (1996).
40. Clementi, E *et al.* Nitric oxide action on growth factor-elicited signals. Phosphoinositide hydrolysis and [Ca^{2+}]i responses are negatively modulated via a cGMP-dependent protein kinase I pathway. *J. Biol. Chem.* **270**, 22277–22282 (1995).
41. Goslin, K., Asmussen, H. & Banker, G. Rat hippocampal neurons in low-density culture. in *Culturing Nerve Cells* (eds. Banker, G. & Goslin, K.) 339–370 (MIT Press, Cambridge, Massachusetts, 1998).
42. Xia, Z., Dudek, H., Miranti, C.K. & Greenberg, M.E. Calcium influx via the NMDA receptor induces immediate early gene transcription by a MAP kinase/ ERK-dependent mechanism. *J. Neurosci.* **16**, 5425–5436 (1996).